



Published in final edited form as:

JAMA Neurol. 2014 June ; 71(6): 725–734. doi:10.1001/jamaneurol.2014.446.

## Emerging $\beta$ -Amyloid Pathology and Accelerated Cortical Atrophy

**Niklas Mattsson, MD, PhD, Philip S. Insel, MS, Rachel Nosheny, PhD, Duygu Tosun, PhD, John Q. Trojanowski, MD, PhD, Leslie M. Shaw, PhD, Clifford R. Jack Jr, MD, Michael C. Donohue, PhD, Michael W. Weiner, MD, and for the Alzheimer's Disease Neuroimaging Initiative**

Department of Veterans Affairs Medical Center, Center for Imaging of Neurodegenerative Diseases, San Francisco, California (Mattsson, Insel, Nosheny, Tosun, Weiner); Clinical Neurochemistry Laboratory, Institute of Neuroscience and Physiology, The Sahlgrenska Academy, University of Gothenburg, Mölndal, Sweden (Mattsson); Department of Radiology and Biomedical Imaging, University of California, San Francisco (Mattsson, Insel, Tosun, Weiner); Department of Pathology and Laboratory Medicine, Institute on Aging, Center for Neurodegenerative Disease Research, Perelman School of Medicine, University of Pennsylvania,

Copyright 2014 American Medical Association. All rights reserved.

Corresponding Author: Niklas Mattsson, MD, PhD, Department of Veterans Affairs Medical Center, Center for Imaging of Neurodegenerative Diseases, Bldg 13, San Francisco, CA 94121, (niklas.mattsson@neuro.gu.se).

Supplemental content at [jamaneurology.com](http://jamaneurology.com)

**Author Contributions:** Dr Mattsson had full access to all the data in the study and takes responsibility for the integrity of the data and the accuracy of the data analysis.

*Study concept and design:* Mattsson, Insel, Nosheny, Tosun, Trojanowski, Weiner.

*Acquisition, analysis, or interpretation data:* Mattsson, Insel, Tosun, Trojanowski, Shaw, Jack, Donohue, Weiner.

*Drafting of the manuscript:* Mattsson, Insel, Tosun, Trojanowski, Weiner.

*Critical revision of the manuscript for important intellectual content:* Insel, Nosheny, Tosun, Trojanowski, Shaw, Jack, Donohue, Weiner.

*Statistical analysis:* Mattsson, Insel, Nosheny, Tosun, Trojanowski, Donohue.

*Obtained funding:* Trojanowski, Weiner.

*Administrative, technical, or material support:* Trojanowski, Shaw, Jack.

*Study supervision:* Tosun, Trojanowski, Weiner.

**Conflict of Interest Disclosures:** Dr Trojanowski may accrue revenue in the future on patents submitted by the University of Pennsylvania on which he is coinventor, has received revenue from the sale of Avid to Eli Lilly and Company as coinventor on imaging-related patents submitted by the University of Pennsylvania, and is the William Maul Measey–Truman G. Schnabel, Jr, MD, Professor of Geriatric Medicine and Gerontology. Dr Shaw previously was a consultant for Innogenetics, collaborates on quality assessment activities as part of the Alzheimer's Disease Neuroimaging Initiative, and serves as a consultant to Janssen Research & Development LLC on biomarker studies. Dr Jack provides consulting services for Siemens Healthcare and Janssen Research & Development LLC, holds the Alexander Family Alzheimer's Disease Research Professorship of the Mayo Foundation, and is the recipient of research grants R01-AG011378, R01-AG041851, R01-AG037551, U01-HL096917, U01-AG032438, and U01-AG024904 from the National Institutes of Health. Dr Weiner has stock options in Synarc Inc and Elan Corporation; serves as an associate editor of *Alzheimer's & Dementia*; has served on scientific advisory boards for Pfizer Inc and BOLT International; has received honoraria from Pfizer Inc, Tohoku University, and Danone Trading BV; has research support from Merck & Co Inc, Avid, the Department of Defense, and the Department of Veterans Affairs; has received funding for travel from Pfizer Inc, the International Conference on Alzheimer's and Parkinson's Diseases, Paul Sabatier University, Novartis, Tohoku University, MCI Group, France, Travel eDreams Inc, Neuroscience School of Advanced Studies, Danone Trading BV, and the Clinical Trials on Alzheimer's Disease ANT Congrès; and has been a consultant for Pfizer Inc, Janssen Research & Development LLC, KLJ Associates, Easton Associates, Harvard University, inThought, INC Research LLC, the Alzheimer's Drug Discovery Foundation, Sanofi Groupe, and the University of California, Los Angeles. No other disclosures were reported.

**Group Information:** A complete list of the ADNI investigators can be found at [http://adni.loni.usc.edu/wp-content/uploads/how\\_to\\_apply/ADNI\\_Acknowledgement\\_List.pdf](http://adni.loni.usc.edu/wp-content/uploads/how_to_apply/ADNI_Acknowledgement_List.pdf). Data used in the preparation of this article were obtained from the ADNI database (<http://adni.loni.usc.edu>). As such, the investigators within the ADNI contributed to the design and implementation of ADNI and/or provided data but did not participate in the analysis or writing of this report.

Philadelphia (Trojanowski, Shaw); Department of Radiology, Mayo Clinic, Rochester, Minnesota (Jack); Division of Biostatistics and Bioinformatics, Department of Family and Preventive Medicine, University of California, San Diego, La Jolla (Donohue)

## Abstract

**Importance**—The effect of  $\beta$ -amyloid ( $A\beta$ ) accumulation on regional structural brain changes in early stages of Alzheimer disease (AD) is not well understood.

**Objective**—To test the hypothesis that the development of  $A\beta$  pathology is related to increased regional atrophy in the brains of cognitively normal (CN) persons.

**Design, Setting, and Participants**—Longitudinal clinicobiomarker cohort study involving 47 CN control subjects and 15 patients with AD dementia. All participants underwent repeated cerebrospinal fluid  $A\beta_{42}$  and structural magnetic resonance imaging measurements for up to 4 years. Cognitively normal controls were classified using the longitudinal cerebrospinal fluid  $A\beta_{42}$  data and included 13 stable  $A\beta$  negative (normal baseline  $A\beta_{42}$  levels, with less than the median reduction over time), 13 declining  $A\beta$  negative (normal baseline  $A\beta_{42}$  levels, with greater than the median reduction over time), and 21  $A\beta$  positive (pathologic baseline  $A\beta_{42}$  levels). All 15 patients with AD dementia were  $A\beta$  positive.

**Main Outcomes and Measures**—Group effects on regional gray matter volumes at baseline and over time, tested by linear mixed-effects models.

**Results**—Baseline gray matter volumes were similar among the CN  $A\beta$  groups, but atrophy rates were increased in frontoparietal regions in the declining  $A\beta$ -negative and  $A\beta$ -positive groups and in amygdala and temporal regions in the  $A\beta$ -positive group.  $A\beta$ -positive patients with AD dementia had further increased atrophy rates in hippocampus and temporal and cingulate regions.

**Conclusions and Relevance**—Emerging  $A\beta$  pathology is coupled to increased frontoparietal (but not temporal) atrophy rates. Atrophy rates peak early in frontoparietal regions but accelerate in hippocampus, temporal, and cingulate regions as the disease progresses to dementia. Early-stage  $A\beta$  pathology may have mild effects on local frontoparietal cortical integrity while effects in temporal regions appear later and accelerate, leading to the atrophy pattern typically seen in AD.

Hallmarks of Alzheimer disease (AD) include  $\beta$ -amyloid ( $A\beta$ ) plaques, neurofibrillary tangles composed of tau proteins, and progressive brain atrophy.<sup>1</sup>  $\beta$ -Amyloid pathology can be measured by an increased signal of amyloid positron emission tomography (PET)<sup>2,3</sup> or by decreased  $A\beta_{42}$  levels in cerebrospinal fluid (CSF)<sup>4,5</sup> and is seen in about one-third of healthy elders,<sup>6,7</sup> appears several years before cognitive symptoms,<sup>8-10</sup> and has been termed *preclinical AD*.<sup>11</sup> It may occur upstream of tau pathology and atrophy,<sup>12-14</sup> but the exact temporospatial relationship among  $A\beta$  plaques, atrophy, and tangles in AD remains unclear. The atrophy is usually believed to begin in the medial temporal lobe before spreading into other parts of temporal and parietal cortex and finally to most association cortex, including the frontal lobe. This model is based in part on magnetic resonance (MR) imaging studies<sup>15-17</sup> showing most robust changes in hippocampus and temporal cortex. The tau pathology probably first appears in entorhinal cortex (or in the brainstem<sup>18,19</sup>) before reaching hippocampus and other parts of temporal and parietal cortex.<sup>20,21</sup> The development of  $A\beta$  pathology is considerably different, with plaques first appearing in cortical regions

distinct from the medial temporal lobe.<sup>22,23</sup> To unite these different observations, it has been suggested that A $\beta$  and tangles may start independently, with temporal lobe tangles also occurring in normal aging.<sup>24</sup> According to this model, AD first causes A $\beta$  deposition in the neocortex and later tangles in the temporal lobe, sometimes on top of age-related tangles.<sup>25</sup> Studies on A $\beta$  and atrophy in cognitively normal (CN) persons have been discordant, with associations between A $\beta$  and atrophy in temporal cortex and hippocampus<sup>26,27</sup> or primarily in other regions, including the frontal lobe,<sup>28-30</sup> or only in control subjects with subjective memory impairment.<sup>31</sup>  $\beta$ -Amyloid pathology has sometimes (but not always<sup>32,33</sup>) been associated with longitudinal atrophy in CN persons in hippocampus and temporal cortex,<sup>34,35</sup> as well as in regions not typically associated with early AD.<sup>36</sup> Finally, A $\beta$  has been associated with larger volume in temporal regions, perhaps indicating brain reserve mechanisms.<sup>37</sup>

Reports of a bimodal distribution of A $\beta$  biomarkers<sup>23,38</sup> suggest that the transition from A $\beta$  negative to A $\beta$  positive may be rapid, making it possible to observe CN elders with no evidence of preclinical AD but with rapidly changing CSF A $\beta$ 42 levels, indicating emerging A $\beta$  pathology. Few studies have simultaneously measured longitudinal biomarkers of A $\beta$  and brain structure in CN persons. A recent study<sup>39</sup> found no difference in hippocampal atrophy rates based on emerging A $\beta$  pathology in CN persons but did not test atrophy in other regions. One possible outcome of such an analysis would be that emerging A $\beta$  pathology is associated with increased atrophy in the temporal lobe, consistent with the usually perceived pattern of atrophy in AD. Alternatively, emerging A $\beta$  pathology might be associated with atrophy in association cortical areas distant from the medial temporal lobe, consistent with local neurotoxic effects of A $\beta$ .<sup>14</sup> Herein, we examined the kinetics of CSF A $\beta$ 42 and brain structure in CN elders. Based on the idea that A $\beta$  may follow a sigmoidal trajectory,<sup>40</sup> we classified individuals into successively more advanced stages using combinations of baseline and longitudinal CSF A $\beta$ 42 measurements (for details, see the Statistical Analysis section of the Methods) as follows: stable A $\beta$  negative (CN A $\beta$ -s), declining A $\beta$  negative (CN A $\beta$ -d), and A $\beta$  positive (CN A $\beta$ +). We also included A $\beta$ -positive patients with AD dementia (AD A $\beta$ +). We tested the hypotheses that the groups differed in gray matter (GM) volumes at baseline and longitudinally.

## Methods

### Participants

Institutional review board approval was obtained from every involved institution, and written informed consent was obtained from the participants. Data were obtained from the Alzheimer's Disease Neuroimaging Initiative (ADNI) database ([adni.loni.usc.edu](http://adni.loni.usc.edu)). The senior author (M.W.W.) is the principal investigator of this initiative. The ADNI is the result of efforts of many coinvestigators, and participants have been recruited from more than 50 sites across the United States and Canada ([www.adni-info.org](http://www.adni-info.org)). The population in this study included ADNI 1 participants who were tested for CSF A $\beta$ 42 levels at multiple time points and had successful longitudinal FreeSurfer (version 4.4; <http://surfer.nmr.mgh.harvard.edu/fswiki>) processing of MR images from at least 2 time points. Results on the cognitive subscale of the Alzheimer Disease Assessment Scale were used to assess cognitive function.

## Structural MR Image Acquisition

Structural brain MR images were acquired at multiple sites using 1.5-T imaging systems ( 6 time points, at screening and at 6, 12, 24, 36, and 48 months) with a standardized protocol that included T1-weighted MR imaging using a sagittal volumetric magnetization-prepared rapid gradient-echo sequence.<sup>41</sup>

## FreeSurfer Longitudinal MR Image Processing

Automated cortical and subcortical volume and thickness measures were performed with FreeSurfer.<sup>42,43</sup> To reduce the confounding effect of intraparticipant morphologic variability, each participant's longitudinal data series was processed by FreeSurfer longitudinal work flow (<http://surfer.nmr.mgh.harvard.edu/fswiki/LongitudinalProcessing>). A previous test-retest study<sup>44</sup> had validated that the longitudinal processing provides consistent region of interest (ROI) segmentation. All images underwent standardized quality control. Participants with complete segmentation failure or gross errors throughout all brain regions were rated as complete failures. Participants with gross errors in 1 or more specific brain regions (ie, temporal lobe regions, superior regions, occipital regions, and insula) were given a partial pass rating. Participants with a partial pass rating were included in analyses of appropriate brain regions only.

The main analysis of this study focused on GM volumes. To reduce the problem of multiple comparisons, we used 6 a priori defined combinations of ROI volumes (overall, temporal, cingulate, parietal, frontal, and occipital regions), plus the individual data for hippocampus and amygdala. For the over all volume, we combined data from all available GM ROIs. For the temporal lobe, we combined the temporal pole, fusiform, superior temporal, inferior temporal, middle temporal, banks of the superior temporal sulcus, transverse temporal, entorhinal, and parahippocampal ROIs. For the cingulate, we combined the rostral anterior cingulate, caudal anterior cingulate, posterior cingulate, and isthmus cingulate ROIs. For the parietal lobe, we combined the postcentral, superior parietal, supramarginal, paracentral, inferior parietal, and precuneus ROIs. For the frontal lobe, we combined the frontal pole, precentral, caudal middle frontal, rostral middle frontal, medial orbitofrontal, pars orbitalis, pars triangularis, pars opercularis, and superior frontal ROIs. For the occipital lobe, we combined the lingual, lateral occipital, pericalcarine, and cuneus ROIs. In a secondary exploratory analysis, we tested all available FreeSurfer GM ROIs individually. Data of the right and left hemispheres were averaged in all analyses. As a supplementary analysis, we also tested effects on cortical thickness instead of GM volume.

## White Matter Hyperintensities and Hypointensities

The presence of vascular disease was a potential confounder for the relationship between amyloid and atrophy. Therefore, we included data for white matter hyperintensities, quantified from structural proton density-weighted, T1-weighted, and T2-weighted MR images as described in detail previously,<sup>45</sup> and data for white matter hypointensities, quantified by automatic volume measurements using FreeSurfer.

## CSF Biomarker Concentrations

Cerebrospinal fluid was acquired annually ( 5 time points, at baseline and at 12, 24, 36, and 48 months) by lumbar puncture and stored at  $-80^{\circ}\text{C}$  at the ADNI Biomarker Core laboratory at the University of Pennsylvania Medical Center.  $\beta$ -Amyloid42, T-tau, and P-tau were measured with a multiplex platform (xMAP; Luminex Corporation) using a kit (INNO-BIA AlzBio3; Innogenetics).<sup>5,46</sup> The biomarker data set (UPENNBBIOMK4.csv; <http://adni.loni.usc.edu/>) has been described previously<sup>38,47,48</sup> but not in relation to MR imaging measurements.

## Excluded Data

From the original CSF data set, one CN individual was excluded because of atypical A $\beta$ 42 data (A $\beta$ 42 levels increased greatly over time), and another CN individual was excluded because of atypical structural data (volumes increased greatly over time in several subcortical regions). Because we wanted to ensure that any differences in structure between the CN A $\beta$ -s and CN A $\beta$ -d groups were caused by emerging rather than established A $\beta$  pathology, we excluded data from individuals crossing the A $\beta$ 42 cutoff of 192 ng/L during the study. This included one individual who had a baseline A $\beta$ 42 level exceeding 192 ng/L but all follow-up A $\beta$ 42 levels less than 192 ng/L (we excluded all data for that individual), as well as data from 3 individuals who had baseline A $\beta$ 42 levels exceeding 192 ng/L but last follow-up (month 36) A $\beta$ 42 levels less than 192 ng/L (we excluded the data from the last visit for those individuals). As described below, we repeated the analyses with all the data included, which did not change the main findings.

## Statistical Analysis

We used linear mixed-effects models with time as a single predictor to derive baseline levels (intercepts) and longitudinal changes (slopes) of A $\beta$ 42. By definition, the CN A $\beta$ -s group had estimated intercepts exceeding 192 ng/L (100% consistent with observed baseline A $\beta$ 42 levels) and estimated change less than the median among all A $\beta$ -negative CN participants. The CN A $\beta$ -d group had intercepts exceeding 192 ng/L and change exceeding the median among all A $\beta$ -negative CN participants. The CN A $\beta$ + and AD A $\beta$ + groups had intercepts of 192 ng/L or less. The cutoff of 192 ng/L is discriminative of brain A $\beta$  pathology in PET imaging<sup>49</sup> and autopsy<sup>5</sup> studies, with samples analyzed at the same laboratory as in the present study.

Therefore, the study contained 4 groups representing increasingly severe stages of A $\beta$  pathology and cognition. These included CN A $\beta$ -s (n = 13), CN A $\beta$ -d (n = 13), CN A $\beta$ + (n = 21), and AD A $\beta$ + (n = 15).

The main objective was to test whether baseline volumes and atrophy rates varied among groups. To test potential confounding factors, we evaluated associations between study group and demographic factors (age, sex, education, apolipoprotein E [*APOE*]  $\epsilon 4$  genotype status, white matter hyperintensities, white matter hypointensities, and history of hypertension) using Kruskal-Wallis tests and  $\chi^2$  tests. The final models were linear mixed-effects models with volume as the response variable and the interaction between time and group (including subeffects) as the main predictor, adjusted for age, sex, education,

intracranial volume, and *APOE*  $\epsilon 4$  genotype status. Differences in baseline volumes were determined by the group effect and differences in atrophy rates by the interaction between time and group. Groups were tested pairwise in 4 combinations (CN A $\beta$ -s vs CN A $\beta$ -d, CN A $\beta$ +, or AD A $\beta$ + and CN A $\beta$ + vs AD A $\beta$ +). We also tested group differences in T-tau and P-tau levels and cognitive subscale scores on the Alzheimer Disease Assessment Scale using linear mixed-effects models. Secondly, we compared atrophy rates among CN A $\beta$  groups in all available GM ROIs to assess whether differences were consistent for individual ROIs within lobes. We used nonparametric bootstrap resamples ( $n = 1000$ ) to generate 95% CIs for the comparisons. As a supplementary analysis, we also analyzed cortical thickness as the response.

We used logistic models to test whether variables were related to study dropout, with age, sex, education, and study group as predictors of missing data (for A $\beta$ 42 levels, we compared individuals with 2-3 data points vs individuals with 4-5 data points; for MR imaging, we created a missing indicator [true or false] for each study visit). All linear mixed-effects models included a random intercept and a random slope. The applicability of the models was assessed by evaluating fitted vs observed measurement within participants, normality of model residuals, and quantile-quantile plots. All tests were 2-sided, and significance was set at  $P < .05$ . Correction for multiple comparisons was performed by the false discovery rate when indicated. All statistical analyses were performed using R (version 3.0.1; The R Foundation for Statistical Computing).

## Results

Study demographics are summarized in the Table. The *APOE*  $\epsilon 4$  genotype status differed between groups (rare in CN A $\beta$ -s and CN A $\beta$ -d but common in CN A $\beta$ + and AD A $\beta$ +). The groups were also not completely balanced on age, sex, and education (range,  $P = .10$  to  $P = .20$ ). Therefore, all models were adjusted for age, sex, education, and *APOE*  $\epsilon 4$  genotype status. Some individuals had a history of hypertension and increased levels of white matter hyperintensities or white matter hypointensities, but because the groups were balanced on these parameters ( $P = .84$ ,  $P = .81$ , and  $P = .41$ , respectively), we did not adjust for them in the final models (although including them did not change the main results [data not shown]).

### Missing Data

Participants lacked some CSF data (1 at baseline, 3 at 12 months, 22 at 24 months, 24 at 36 months, and 47 at 48 months) or MR imaging (2 at baseline, 4 at 6 months, 4 at 12 months, 11 at 24 months, 33 at 36 months, and 54 at 48 months). Study group effects were not associated with missing data.

### Baseline Volumes in A Priori Regions

No differences were observed among CN groups in baseline volumes in the a priori defined regions (Figure 1). The AD A $\beta$ + group had smaller overall, hippocampus, amygdala, temporal, and parietal volumes compared with the CN A $\beta$ -s group and had smaller overall, hippocampus, amygdala, temporal, cingulate, and parietal volumes compared with the CN A $\beta$ + group.

### Atrophy Rates in A Priori Regions

Compared with the CN A $\beta$ -s group, the CN A $\beta$ -d group had increased atrophy rates in the overall, frontal, and parietal regions, and the CN A $\beta$ + group had increased atrophy rates in the overall, amygdala, temporal, cingulate, frontal, and parietal regions (Figure 2). The AD A $\beta$ + group had increased atrophy rates in all regions compared with the CN A $\beta$ -s group and had increased atrophy rates in overall, hippocampus, temporal, and cingulate regions compared with the CN A $\beta$ + group.

### Group Differences in Atrophy Rates in All ROIs

We compared atrophy rates among CN groups in all available ROIs using group resampling and nonparametric bootstrapping to estimate 95% CIs. Regions within lobes often had similarly altered atrophy rates (Figure 3). The CN A $\beta$ -d group had increased atrophy rates compared with the CN A $\beta$ -s group predominantly in frontoparietal regions, while most temporal, cingulate, occipital, and subcortical regions had similar rates between these groups (Figure 3, left). The CN A $\beta$ + group had increased rates compared with the CN A $\beta$ -s group in most regions, with largest effects in amygdala and several parietal, temporal (but not hippocampus), and frontal regions (Figure 3, middle). The CN A $\beta$ + group also had increased rates compared with the CN A $\beta$ -d group predominantly in amygdala and temporal lobe regions but not in frontoparietal or most cingulate regions (Figure 3, right).

### Analyses of Cortical Thickness

As a supplementary analysis, we also tested for differences in cortical thickness in the overall brain and in lobes (eFigure 1 and eFigure 2 in the Supplement). The results were similar to the results for volume. The main difference was that the rates of atrophy were slightly less pronounced in the CN A $\beta$ + group compared with the CN A $\beta$ -s group than in the volume analysis, but rates remained significantly increased in the parietal lobe.

### A $\beta$ Pathology and Cognition

Baseline cognitive subscale scores on the Alzheimer Disease Assessment Scale were similar between the CN A $\beta$ -s and CN A $\beta$ -d groups, but the CN A $\beta$ + group had a trend for higher scores than the CN A $\beta$ -s group (Table). Longitudinal cognitive subscale changes on the Alzheimer Disease Assessment Scale were smallest in the CN A $\beta$ -s group and greater in the CN A $\beta$ -d and CN A $\beta$ + groups (significantly different compared with the CN A $\beta$ -s group). As expected, the AD A $\beta$ + group had higher baseline scores and increases over time compared with CN participants.

### A $\beta$ Pathology and Tau Biomarkers

Baseline T-tau and P-tau levels were similar between the CN A $\beta$ -s and CN A $\beta$ -d groups but were greater in the CN A $\beta$ + and AD A $\beta$ + groups (Table). Slopes of T-tau and P-tau were similar between groups but showed trends to greater levels in the CN A $\beta$ + and AD A $\beta$ + groups (significant for AD and P-tau).

## Discussion

Our main findings were (1) a subset of CN participants with CSF A $\beta$ 42 levels in the normal range (and no preclinical AD by current definitions<sup>11</sup>) demonstrates longitudinal CSF A $\beta$ 42 reductions coupled to increased frontoparietal cortical atrophy rates in the absence of accelerated temporal atrophy and (2) CN participants with reduced CSF A $\beta$ 42 levels at baseline have widespread increased cortical atrophy rates in addition to the frontoparietal regions. Our results suggest a stage of emerging amyloid pathology in CN persons before the presence of widespread amyloid plaques, which is associated with frontoparietal cortical thinning that does not accelerate further during the disease progression. Once individuals have evidence of widespread cortical plaque pathology, they also show signs of accelerating atrophy in regions usually considered to be affected by atrophy in AD.

The finding that frontoparietal atrophy rates were increased in the CN A $\beta$ -d group is novel. A recently published study<sup>39</sup> used a similar approach but only tested atrophy rates in hippocampus, where there were no differences between controls in various A $\beta$  groups (consistent with our results). Previous investigations examining correlations between A $\beta$  pathology and brain structure in controls have been discrepant, with some reports of associations between atrophy and A $\beta$  pathology,<sup>26,27,34,50,51</sup> associations only in controls with subjective cognitive impairment,<sup>31,37</sup> or associations only in individuals with concomitant increased P-tau levels<sup>52</sup> or other signs of brain injury.<sup>53</sup> Several of these studies<sup>34,53</sup> found increased atrophy rates in the temporal lobe in the presence of A $\beta$  pathology, consistent with our results for the CN A $\beta$ + group. Our results are also in line with previous findings of association between A $\beta$  pathology and atrophy in parietal and frontal regions in healthy controls.<sup>29,30</sup>

Frontoparietal regions are known to be sites of early A $\beta$  deposition, and although the CSF A $\beta$ 42 measurements in this study provide no information on regional A $\beta$  pathology, it is possible that localized A $\beta$  pathology was coupled to early effects on frontoparietal structures.<sup>31</sup> The fact that the CN A $\beta$ -s and CN A $\beta$ -d groups had similar levels of T-tau and P-tau, which are believed to indicate AD-type axonal degeneration and neurofibrillary tangles,<sup>54</sup> may suggest that the increased atrophy rates in the CN A $\beta$ -d group were partly tau independent. However, autopsy studies show that severe A $\beta$ -associated neurodegeneration is rare in the absence of tangles<sup>55</sup> or other pathologies.<sup>56</sup> One possibility in the present study is that local A $\beta$  (fibrils or oligomers) damaged cortical cells, but it is unclear if this occurs without concurrent tau pathology.<sup>57</sup> Neocortical tau deposition may be present in CN persons,<sup>58</sup> making it possible that the increased atrophy rates found herein occurred on a background of tau or other brain pathology. We considered the possibility that vascular pathology confounded our findings. Some individuals had increased white matter hyperintensities or hypointensities or a history of hypertension. However, the groups were balanced on all these parameters, and adjusting for them did not change the main results (data not shown).

Our finding that the CN A $\beta$ + group had increased atrophy rates not only in frontoparietal regions but also in amygdala, temporal, and cingulate regions supports the notion that A $\beta$  accumulation induces atrophy in different brain regions at various stages. The CN A $\beta$ + and



AD A $\beta$ + groups had similar atrophy rates in amygdala, indicating that atrophy there peaks early. In contrast, atrophy rates in hippocampus, temporal, and cingulated regions were greater in the AD A $\beta$ + group compared with the CN A $\beta$ + group, indicating accelerated atrophy as the disease becomes symptomatic.

Our main limitation was the small sample size, especially for comparing the CN A $\beta$ -s and CN A $\beta$ -d groups. The classification of A $\beta$ -negative CN participants as stable vs declining using a median split of the A $\beta$ 42 slope does not exclude an overlap in pathology for individuals with intermediate A $\beta$ 42 changes. However, the overall results remained significant or close to significant when we excluded the mid-tertile (8 of 26) of A $\beta$ -negative CN participants with intermediate changes, supporting our main conclusions (data not shown). Another limitation is that we did not determine the presence of other potentially important brain pathologies, including mild tau pathology, hippocampal sclerosis, Lewy bodies, or TDP-43 inclusions,<sup>56,59</sup> which may have affected brain atrophy rates. As explained above, we excluded a few individuals with atypical A $\beta$ 42 measurements, but the main results were stable when we included all individuals and data (eFigure 3 and eFigure 4 in the Supplement). A slight imbalance was observed in the proportions of men and women between groups, but all models were adjusted for sex. A final limitation concerns the measurement variability of CSF biomarkers, which may potentially introduce artificial changes.<sup>60</sup> The intraassay coefficient of variation for CSF A $\beta$ 42 was 10.5% or less (all samples from each individual run at the same plate). However, this variability is not biased toward reduced levels over time, and we included 3 or 4 CSF measurements for most individuals, which greatly increase the robustness of the estimates compared with estimating slopes from only 2 time points.

## Conclusions

In summary, we identify a group of CN persons with emerging amyloid pathology coupled to increased atrophy rates in frontoparietal but not temporal regions, suggesting local effects on brain structure during early stages of A $\beta$  accumulation. Cognitively normal participants and patients having AD with signs of widespread A $\beta$  pathology had increased atrophy rates in classic AD regions. Our results modify previous models of the relationship between A $\beta$  and regional atrophy during the development of AD.

## Supplementary Material

Refer to Web version on PubMed Central for supplementary material.

## Acknowledgments

**Funding/Support:** Data collection and sharing for this project were funded by grant U01-AG024904 from the National Institutes of Health to the Alzheimer's Disease Neuroimaging Initiative (ADNI). The ADNI is funded by the National Institute on Aging, the National Institute of Biomedical Imaging and Bioengineering, and through generous contributions from Abbott, AstraZeneca AB, Bayer Schering Pharma AG, Bristol-Myers Squibb, Eisai Global Clinical Development, Elan Corporation, Genentech, GE Healthcare, GlaxoSmithKline, Innogenetics, Johnson & Johnson, Eli Lilly and Company, Medpace Inc, Merck and Co Inc, Novartis AG, Pfizer Inc, F. Hoffman–La Roche, Schering-Plough, and Synarc Inc, as well as by its nonprofit partners the Alzheimer's Association and the Alzheimer's Drug Discovery Foundation, with participation from the US Food and Drug Administration. Private sector contributions to the ADNI are facilitated by the Foundation for the National Institutes of Health ([www.fnih.org](http://www.fnih.org)). The grantee organization is the Northern California Institute for Research and

Education, and the study is coordinated by the Alzheimer's Disease Cooperative Study at the University of California, San Diego. The ADNI data are disseminated by the Laboratory for Neuro Imaging at the University of California, Los Angeles. This research was also supported by grants P30-AG010129 and K01-AG030514 from the National Institutes of Health, the Swedish Research Council, Goteborgs Lakaresallskap, Svenska Lakaresallskapet, Sahlgrenska Universitetssjukhuset, Carl-Bertil Laurells Fond, and Klinisk Biokemi i Norden.

**Role of the Sponsor:** The funding sources had no role in the design and conduct of the study; collection, management, analysis, and interpretation of the data; preparation, review, or approval of the manuscript; and decision to submit the manuscript for publication.

## References

1. Blennow K, de Leon MJ, Zetterberg H. Alzheimer's disease. *Lancet*. 2006; 368(9533):387–403. [PubMed: 16876668]
2. Choi SR, Schneider JA, Bennett DA, et al. Correlation of amyloid PET ligand florbetapir F 18 (<sup>18</sup>F-AV-45) binding with  $\beta$ -amyloid aggregation and neuritic plaque deposition in postmortem brain tissue. *Alzheimer Dis Assoc Disord*. 2012; 26(1):8–16. [PubMed: 22354138]
3. Clark CM, Pontecorvo MJ, Beach TG, et al. AV-45-A16 Study Group. Cerebral PET with florbetapir compared with neuropathology at autopsy for detection of neuritic amyloid- $\beta$  plaques: a prospective cohort study. *Lancet Neurol*. 2012; 11(8):669–678. published correction appears in *Lancet Neurol*. 2012;11(8):658. [PubMed: 22749065]
4. Strozyk D, Blennow K, White LR, Launer LJ. CSF A $\beta$  42 levels correlate with amyloid-neuropathology in a population-based autopsy study. *Neurology*. 2003; 60(4):652–656. [PubMed: 12601108]
5. Shaw LM, Vanderstichele H, Knapik-Czajka M, et al. Alzheimer's Disease Neuroimaging Initiative. Cerebrospinal fluid biomarker signature in Alzheimer's Disease Neuroimaging Initiative subjects. *Ann Neurol*. 2009; 65(4):403–413. [PubMed: 19296504]
6. Arriagada PV, Marzloff K, Hyman BT. Distribution of Alzheimer-type pathologic changes in nondemented elderly individuals matches the pattern in Alzheimer's disease. *Neurology*. 1992; 42(9):1681–1688. [PubMed: 1307688]
7. Morris JC, Storandt M, McKeel DW Jr, et al. Cerebral amyloid deposition and diffuse plaques in “normal” aging: evidence for presymptomatic and very mild Alzheimer's disease. *Neurology*. 1996; 46(3):707–719. [PubMed: 8618671]
8. Bateman RJ, Xiong C, Benzinger TL, et al. Dominantly Inherited Alzheimer Network. Clinical and biomarker changes in dominantly inherited Alzheimer's disease. *N Engl J Med*. 2012; 367(9):795–804. [PubMed: 22784036]
9. Jack CR Jr, Knopman DS, Jagust WJ, et al. Hypothetical model of dynamic biomarkers of the Alzheimer's pathological cascade. *Lancet Neurol*. 2010; 9(1):119–128. [PubMed: 20083042]
10. Vos SJ, Xiong C, Visser PJ, et al. Preclinical Alzheimer's disease and its outcome: a longitudinal cohort study. *Lancet Neurol*. 2013; 12(10):957–965. [PubMed: 24012374]
11. Sperling RA, Aisen PS, Beckett LA, et al. Toward defining the preclinical stages of Alzheimer's disease: recommendations from the National Institute on Aging–Alzheimer's Association workgroups on diagnostic guidelines for Alzheimer's disease. *Alzheimers Dement*. 2011; 7(3): 280–292. [PubMed: 21514248]
12. Hardy JA, Higgins GA. Alzheimer's disease: the amyloid cascade hypothesis. *Science*. 1992; 256(5054):184–185. [PubMed: 1566067]
13. Selkoe DJ. Resolving controversies on the path to Alzheimer's therapeutics. *Nat Med*. 2011; 17(9): 1060–1065. [PubMed: 21900936]
14. Benilova I, Karran E, De Strooper B. The toxic A $\beta$  oligomer and Alzheimer's disease: an emperor in need of clothes. *Nat Neurosci*. 2012; 15(3):349–357. [PubMed: 22286176]
15. de Leon MJ, George AE, Stylopoulos LA, Smith G, Miller DC. Early marker for Alzheimer's disease: the atrophic hippocampus. *Lancet*. 1989; 2(8664):672–673. [PubMed: 2570916]
16. Singh V, Chertkow H, Lerch JP, Evans AC, Dorr AE, Kabani NJ. Spatial patterns of cortical thinning in mild cognitive impairment and Alzheimer's disease. *Brain*. 2006; 129(pt 11):2885–2893. [PubMed: 17008332]

17. Fjell AM, Walhovd KB, Fennema-Notestine C, et al. Alzheimer's Disease Neuroimaging Initiative. CSF biomarkers in prediction of cerebral and clinical change in mild cognitive impairment and Alzheimer's disease. *J Neurosci*. 2010; 30(6):2088–2101. [PubMed: 20147537]
18. Braak H, Del Tredici K. Reply: the early pathological process in sporadic Alzheimer's disease. *Acta Neuropathol*. 2013; 126(4):615–618. [PubMed: 23982593]
19. Attems J, Jellinger KA. Amyloid and tau: neither chicken nor egg but two partners in crime! *Acta Neuropathol*. 2013; 126(4):619–621. [PubMed: 23955601]
20. Tomlinson BE, Blessed G, Roth M. Observations on the brains of demented old people. *J Neurol Sci*. 1970; 11(3):205–242. [PubMed: 5505685]
21. Braak H, Braak E. Neuropathological staging of Alzheimer-related changes. *Acta Neuropathol*. 1991; 82(4):239–259. [PubMed: 1759558]
22. Thal DR, Rüb U, Orantes M, Braak H. Phases of A $\beta$ -deposition in the human brain and its relevance for the development of AD. *Neurology*. 2002; 58(12):1791–1800. [PubMed: 12084879]
23. Mintun MA, Larossa GN, Sheline YI, et al. [<sup>11</sup>C]PIB in a nondemented population: potential antecedent marker of Alzheimer disease. *Neurology*. 2006; 67(3):446–452. [PubMed: 16894106]
24. Braak H, Del Tredici K. The pathological process underlying Alzheimer's disease in individuals under thirty. *Acta Neuropathol*. 2011; 121(2):171–181. [PubMed: 21170538]
25. Mungas D, Tractenberg R, Schneider JA, Crane PK, Bennett DA. A 2-process model for neuropathology of Alzheimer's disease. *Neurobiol Aging*. 2014; 35(2):301–308. [PubMed: 24080173]
26. Mormino EC, Kluth JT, Madison CM, et al. Alzheimer's Disease Neuroimaging Initiative. Episodic memory loss is related to hippocampal-mediated  $\beta$ -amyloid deposition in elderly subjects. *Brain*. 2009; 132(pt 5):1310–1323. [PubMed: 19042931]
27. Jack CR Jr, Lowe VJ, Senjem ML, et al. <sup>11</sup>C PiB and structural MRI provide complementary information in imaging of Alzheimer's disease and amnesic mild cognitive impairment. *Brain*. 2008; 131(pt 3):665–680. [PubMed: 18263627]
28. Desikan RS, Sabuncu MR, Schmansky NJ, et al. Alzheimer's Disease Neuroimaging Initiative. Selective disruption of the cerebral neocortex in Alzheimer's disease. *PLoS One*. 2010; 5(9):e12853.10.1371/journal.pone.0012853 [PubMed: 20886094]
29. Becker JA, Hedden T, Carmasin J, et al. Amyloid- $\beta$  associated cortical thinning in clinically normal elderly. *Ann Neurol*. 2011; 69(6):1032–1042. [PubMed: 21437929]
30. Oh H, Habeck C, Madison C, Jagust W. Covarying alterations in A $\beta$  deposition, glucose metabolism, and gray matter volume in cognitively normal elderly. *Hum Brain Mapp*. 2014; 35(1):297–308. [PubMed: 22965806]
31. Chételat G, Villemagne VL, Bourgeat P, et al. Australian Imaging Biomarkers and Lifestyle Research Group. Relationship between atrophy and  $\beta$ -amyloid deposition in Alzheimer disease. *Ann Neurol*. 2010; 67(3):317–324. [PubMed: 20373343]
32. Henneman WJ, Vrenken H, Barnes J, et al. Baseline CSF p-tau levels independently predict progression of hippocampal atrophy in Alzheimer disease. *Neurology*. 2009; 73(12):935–940. [PubMed: 19770469]
33. Tosun D, Schuff N, Shaw LM, Trojanowski JQ, Weiner MW. Alzheimer's Disease Neuroimaging Initiative. Relationship between CSF biomarkers of Alzheimer's disease and rates of regional cortical thinning in ADNI data. *J Alzheimers Dis*. 2011; 26(suppl 3):77–90. [PubMed: 21971452]
34. Chételat G, Villemagne VL, Villain N, et al. AIBL Research Group. Accelerated cortical atrophy in cognitively normal elderly with high  $\beta$ -amyloid deposition. *Neurology*. 2012; 78(7):477–484. [PubMed: 22302548]
35. Schott JM, Bartlett JW, Fox NC, Barnes J. Alzheimer's Disease Neuroimaging Initiative Investigators. Increased brain atrophy rates in cognitively normal older adults with low cerebrospinal fluid A $\beta$ 1-42. *Ann Neurol*. 2010; 68(6):825–834. [PubMed: 21181717]
36. Fjell AM, Walhovd KB, Fennema-Notestine C, et al. Alzheimer's Disease Neuroimaging Initiative. Brain atrophy in healthy aging is related to CSF levels of A $\beta$ 1-42. *Cereb Cortex*. 2010; 20(9):2069–2079. [PubMed: 20051356]

37. Chételat G, Villemagne VL, Pike KE, et al. Australian Imaging Biomarkers and Lifestyle Study of Ageing (AIBL) Research Group. Larger temporal volume in elderly with high versus low beta-amyloid deposition. *Brain*. 2010; 133(11):3349–3358. [PubMed: 20739349]
38. Toledo JB, Xie SX, Trojanowski JQ, Shaw LM. Longitudinal change in CSF tau and A $\beta$  biomarkers for up to 48 months in ADNI. *Acta Neuropathol*. 2013; 126(5):659–670. [PubMed: 23812320]
39. Jack CR Jr, Wiste HJ, Weigand SD, et al. Amyloid-first and neurodegeneration-first profiles characterize incident amyloid PET positivity. *Neurology*. 2013; 81(20):1732–1740. [PubMed: 24132377]
40. Jack CR Jr, Knopman DS, Jagust WJ, et al. Tracking pathophysiological processes in Alzheimer's disease: an updated hypothetical model of dynamic biomarkers. *Lancet Neurol*. 2013; 12(2):207–216. [PubMed: 23332364]
41. Jack CR Jr, Bernstein MA, Fox NC, et al. The Alzheimer's Disease Neuroimaging Initiative (ADNI): MRI methods. *J Magn Reson Imaging*. 2008; 27(4):685–691. [PubMed: 18302232]
42. Fischl B, van der Kouwe A, Destrieux C, et al. Automatically parcellating the human cerebral cortex. *Cereb Cortex*. 2004; 14(1):11–22. [PubMed: 14654453]
43. Fischl B, Salat DH, Busa E, et al. Whole brain segmentation: automated labeling of neuroanatomical structures in the human brain. *Neuron*. 2002; 33(3):341–355. [PubMed: 11832223]
44. Reuter M, Schmansky NJ, Rosas HD, Fischl B. Within-subject template estimation for unbiased longitudinal image analysis. *Neuroimage*. 2012; 61(4):1402–1418. [PubMed: 22430496]
45. Schwarz C, Fletcher E, DeCarli C, Carmichael O. Fully-automated white matter hyperintensity detection with anatomical prior knowledge and without FLAIR. *Inf Process Med Imaging*. 2009; 21:239–251. [PubMed: 19694267]
46. Olsson A, Vanderstichele H, Andreassen N, et al. Simultaneous measurement of  $\beta$ -amyloid<sub>1-42</sub>, total tau, and phosphorylated tau (Thr181) in cerebrospinal fluid by the xMAP technology. *Clin Chem*. 2005; 51(2):336–345. [PubMed: 15563479]
47. Mattsson N, Insel P, Nosheny R, et al. Alzheimer's Disease Neuroimaging Initiative. CSF protein biomarkers predicting longitudinal reduction of CSF  $\beta$ -amyloid<sub>42</sub> in cognitively healthy elders. *Transl Psychiatry*. 2013; 3:e293.10.1038/tp.2013.69 [PubMed: 23962923]
48. Landau SM, Lu M, Joshi AD, et al. Alzheimer's Disease Neuroimaging Initiative. Comparing positron emission tomography imaging and cerebrospinal fluid measurements of  $\beta$ -amyloid. *Ann Neurol*. 2013; 74(6):826–836. [PubMed: 23536396]
49. Weigand SD, Vemuri P, Wiste HJ, et al. Transforming CSF A $\beta$ <sub>42</sub> measures into calculated Pittsburgh Compound B (PIBcalc) units of brain A $\beta$  amyloid. *Alzheimers Dement*. 2011; 7(2):133–141. [PubMed: 21282074]
50. Storandt M, Mintun MA, Head D, Morris JC. Cognitive decline and brain volume loss as signatures of cerebral amyloid- $\beta$  peptide deposition identified with Pittsburgh compound B: cognitive decline associated with A $\beta$  deposition. *Arch Neurol*. 2009; 66(12):1476–1481. [PubMed: 20008651]
51. Bourgeat P, Chételat G, Villemagne VL, et al. AIBL Research Group.  $\beta$ -Amyloid burden in the temporal neocortex is related to hippocampal atrophy in elderly subjects without dementia. *Neurology*. 2010; 74(2):121–127. [PubMed: 20065247]
52. Desikan RS, McEvoy LK, Thompson WK, et al. Alzheimer's Disease Neuroimaging Initiative. Amyloid- $\beta$ -associated clinical decline occurs only in the presence of elevated p-tau. *Arch Neurol*. 2012; 69(6):709–713. [PubMed: 22529247]
53. Knopman DS, Jack CR Jr, Wiste HJ, et al. Selective worsening of brain injury biomarker abnormalities in cognitively normal elderly persons with  $\beta$ -amyloidosis. *JAMA Neurol*. 2013; 70(8):1030–1038. [PubMed: 23797806]
54. Blennow K, Hampel H, Weiner M, Zetterberg H. Cerebrospinal fluid and plasma biomarkers in Alzheimer disease. *Nat Rev Neurol*. 2010; 6(3):131–144. [PubMed: 20157306]
55. Price JL, Morris JC. Tangles and plaques in nondemented aging and “preclinical” Alzheimer's disease. *Ann Neurol*. 1999; 45(3):358–368. [PubMed: 10072051]

56. Wilson RS, Yu L, Trojanowski JQ, et al. TDP-43 pathology, cognitive decline, and dementia in old age. *JAMA Neurol.* 2013; 70(11):1418–1424. [PubMed: 24080705]
57. Klyubin I, Cullen WK, Hu NW, Rowan MJ. Alzheimer's disease A $\beta$  assemblies mediating rapid disruption of synaptic plasticity and memory. *Mol Brain.* 2012; 5:25.10.1186/1756-6606-5-25 [PubMed: 22805374]
58. Price JL, McKeel DW Jr, Buckles VD, et al. Neuropathology of nondemented aging: presumptive evidence for preclinical Alzheimer disease. *Neurobiol Aging.* 2009; 30(7):1026–1036. [PubMed: 19376612]
59. Jellinger KA, Attems J. Neuropathology and general autopsy findings in nondemented aged subjects. *Clin Neuropathol.* 2012; 31(2):87–98. [PubMed: 22385790]
60. Mattsson N, Andreasson U, Persson S, et al. Alzheimer's Association QC Program Work Group. CSF biomarker variability in the Alzheimer's Association quality control program. *Alzheimers Dement.* 2013; 9(3):251–261. [PubMed: 23622690]

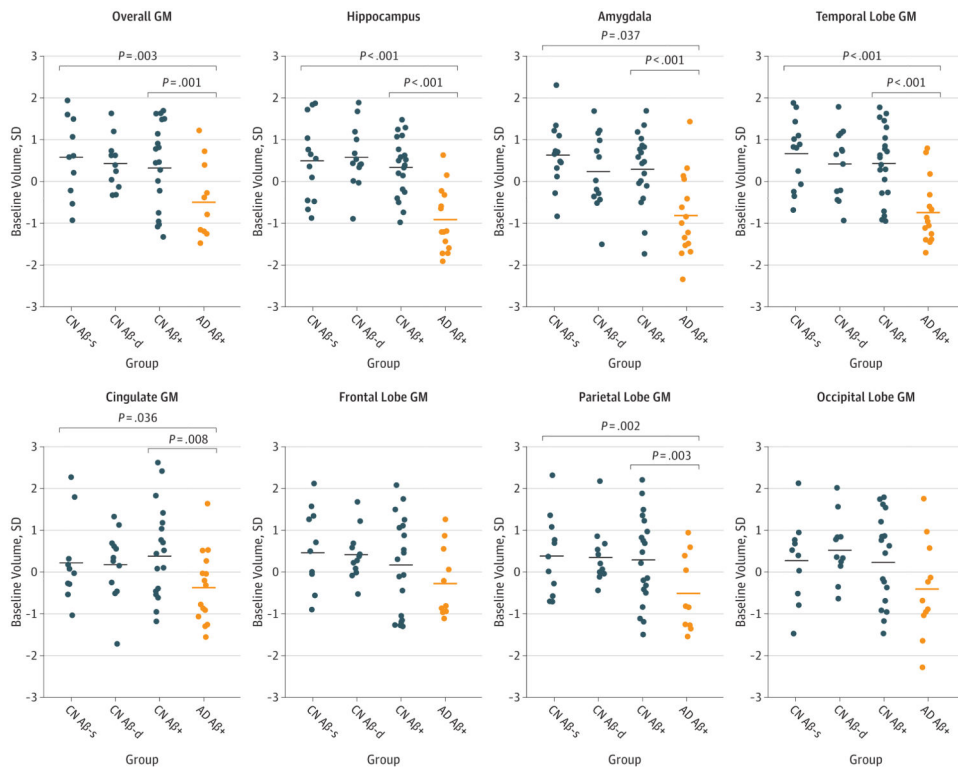


**Figure 1. Baseline Volumes in A Priori Defined Gray Matter (GM) Regions**

Shown are baseline volumes in the study groups. Volumes are centered and standardized. Baseline volumes are modeled data from linear mixed-effects models (intercepts), adjusted for age, sex, education, *APOE ε4* genotype status, and intracranial volume. Horizontal lines are mean values. Significances are indicated for the group effects (pairwise comparisons, comparing every group with the CN Aβ-s group and comparing the AD Aβ+ group with the CN Aβ+ group). When correcting for multiple comparisons (false discovery rate), differences that remained significant were amygdala (CN Aβ+ vs AD Aβ+ [ $P < .001$ ]), cingulate GM (CN Aβ+ vs AD Aβ+ [ $P < .05$ ]), overall GM (CN Aβ-s vs AD Aβ+ [ $P < .05$ ] and CN Aβ+ vs AD Aβ+ [ $P < .05$ ]), hippocampus (CN Aβ-s vs AD Aβ+ [ $P < .01$ ] and CN Aβ+ vs AD Aβ+ [ $P < .001$ ]), temporal lobe GM (CN Aβ-s vs AD Aβ+ [ $P < .001$ ] and CN Aβ+ vs AD Aβ+ [ $P < .001$ ]), and parietal lobe GM (CN Aβ-s vs AD Aβ+ [ $P < .05$ ] and CN Aβ+ vs AD Aβ+ [ $P < .05$ ]). Aβ indicates β-amyloid; AD, Alzheimer disease; AD Aβ+, Aβ-positive AD group; *APOE*, apolipoprotein E; CN, cognitively normal; CN Aβ+, Aβ-positive CN group; CN Aβ-d, declining Aβ-negative CN group; and CN Aβ-s, stable Aβ-negative CN group.

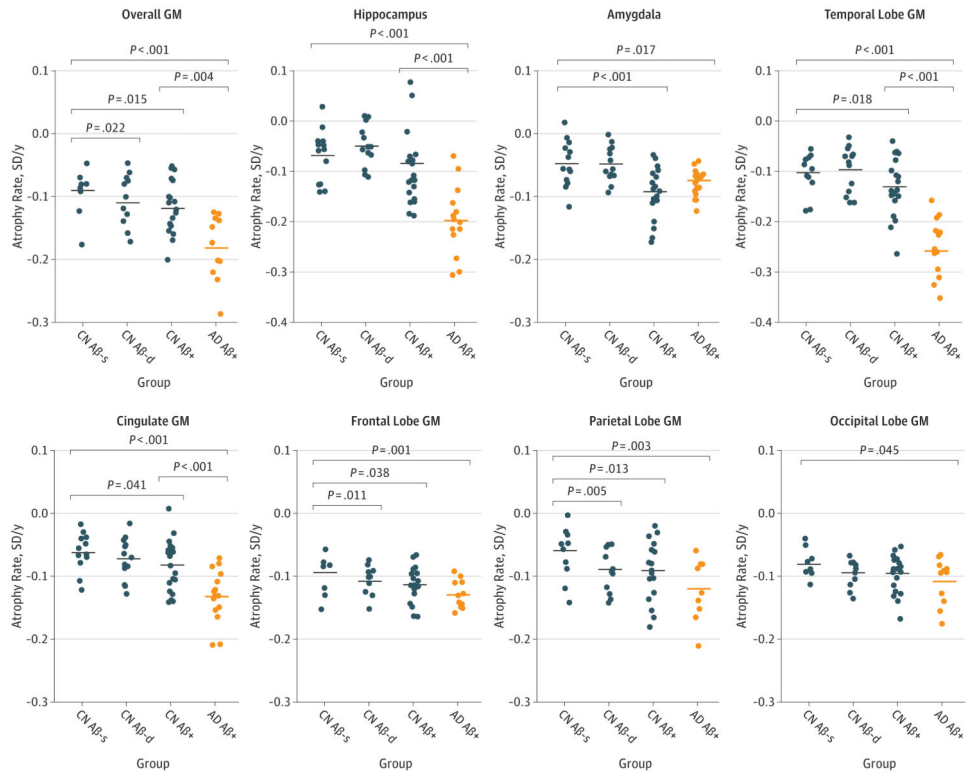


**Figure 2. Atrophy Rates in A Priori Defined Gray Matter (GM) Regions**

Shown are atrophy rates in the study groups. Volumes are centered and standardized.

Atrophy rates are modeled data from linear mixed-effects models (slopes), adjusted for age, sex, education, *APOE*  $\epsilon 4$  genotype status, and intracranial volume. Horizontal lines are mean values. Significances are indicated for the effects of interaction between time and group (pairwise comparisons, comparing every group with the CN Aβ-s group and comparing the AD Aβ+ group with the CN Aβ+ group). When correcting for multiple comparisons (false discovery rate), differences that remained significant were occipital GM (CN Aβ-s vs AD Aβ+ [ $P < .05$ ]), hippocampus (CN Aβ-s vs AD Aβ+ [ $P < .001$ ] and CN Aβ+ vs AD Aβ+ [ $P < .01$ ]), amygdala (CN Aβ-s vs CN Aβ+ [ $P < .01$ ] and CN Aβ-s vs AD Aβ+ [ $P < .05$ ]), frontal GM (CN Aβ-s vs CN Aβ-d [ $P < .05$ ] and CN Aβ-s vs AD Aβ+ [ $P < .01$ ]), cingulate GM (CN Aβ-s vs AD Aβ+ [ $P < .001$ ] and CN Aβ+ vs AD Aβ+ [ $P < .001$ ]), temporal GM (CN Aβ-s vs CN Aβ+ [ $P < .05$ ], CN Aβ-s vs AD Aβ+ [ $P < .001$ ], and CN Aβ+ vs AD Aβ+ [ $P < .001$ ]), parietal GM (CN Aβ-s vs CN Aβ-d [ $P < .05$ ], CN Aβ-s vs CN Aβ+ [ $P < .05$ ], and CN Aβ-s vs AD Aβ+ [ $P < .01$ ]), and overall GM (CN Aβ-s vs CN Aβ-d [ $P < .05$ ], CN Aβ-s vs CN Aβ+ [ $P < .05$ ], CN Aβ-s vs AD Aβ+ [ $P < .001$ ], and CN Aβ+ vs AD Aβ+ [ $P < .05$ ]). Aβ indicates β-amyloid; AD, Alzheimer disease; AD Aβ+, Aβ-positive AD group; *APOE*, apolipoprotein E; CN, cognitively normal; CN Aβ+, Aβ-positive CN group; CN Aβ-d, declining Aβ-negative CN group; and CN Aβ-s, stable Aβ-negative CN group.

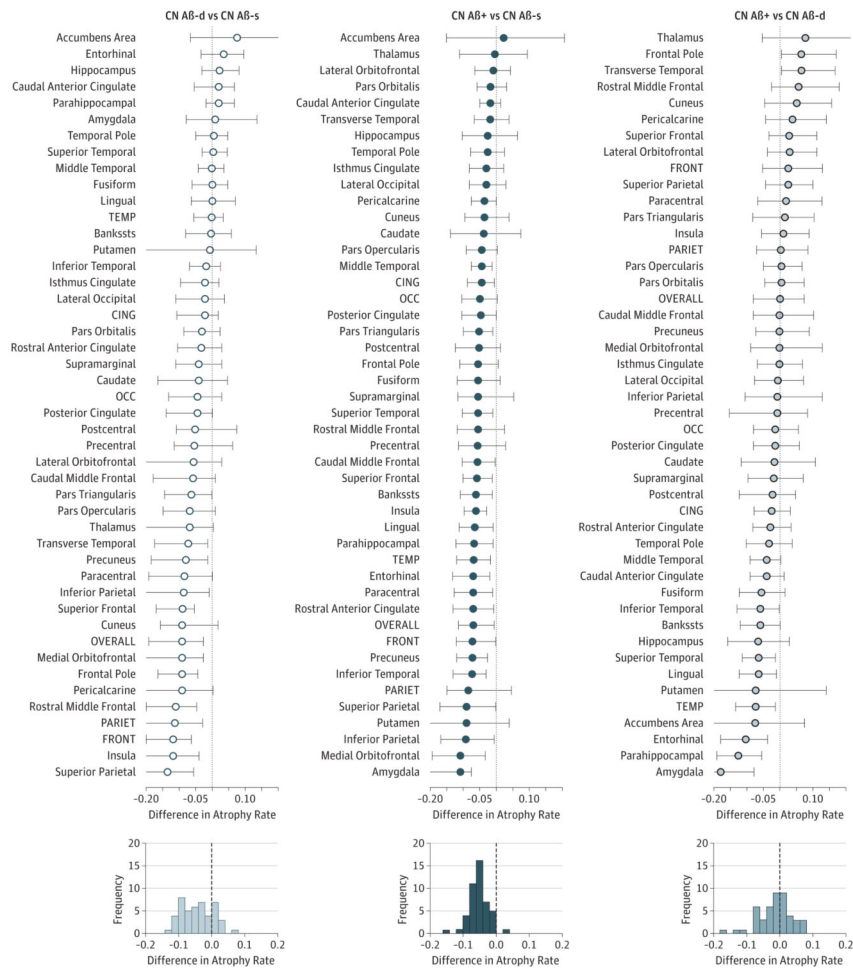


**Figure 3. Comparison of Atrophy Rates Among Groups in All Gray Matter Regions**

The top 3 panels show forest plots of differences in atrophy rates for group comparisons. For each region of interest, the effect of group (from linear mixed models, adjusted for age and sex) is indicated. The 95% CIs were generated by bootstrapping (n = 1000) with resampling of participants. The bottom 3 panels show histograms of the group differences. Note that the same individuals are represented multiple times in this figure because each CN Aβ group is included in 2 comparisons. Volumes were centered and standardized. Combinations of regions were defined as described in the Methods section. Aβ indicates β-amyloid; AD, Alzheimer disease; AD Aβ+, Aβ-positive AD group; Bankssts, banks of the superior temporal sulcus; CING, cingulate regions; CN, cognitively normal; CN Aβ+, Aβ-positive CN group; CN Aβ-d, declining Aβ-negative CN group; CN Aβ-s, stable Aβ-negative CN group; FRONT, frontal regions; OCC, occipital regions; OVERALL, all gray matter regions; PARIET, parietal regions; and TEMP, temporal regions.



Study Demographics<sup>a</sup>

Table

Group	No.	Male-Female Ratio	Age, Mean (SD), y	Education, Mean (SD), y	Positive APOE ε4 Genotype Status, No.	WM Hypertensities, Mean (SD), mL	WM Hypotensities, Mean (SD), mL	History of Hypertension, No.	Cognitive Subscale of the Alzheimer Disease Assessment Scale, Mean (SD)			Aβ42 Level, Mean (SD)		T-tau Level, Mean (SD)		P-tau Level, Mean (SD)	
									Baseline Score	Slope, Units/y	Slope, ng/L* <sup>b</sup>	Baseline, ng/L	Slope, ng/L* <sup>b</sup>	Baseline, ng/L	Slope, ng/L* <sup>b</sup>	Baseline, ng/L	Slope, ng/L* <sup>b</sup>
CN Aβ-s	13	10:3	76.2 (4.8)	16.7 (2.5)	0	0.24 (0.17)	3.8 (1.3)	6	5.2 (0.9)	-0.19 (0.31)	258 (25)	-2.1 (-1.3)	58 (23)	1.8 (0.13)	21 (5.6)	1.8 (1.0)	
CN Aβ-d	13	5:8	78.1 (6.8)	15.2 (2.5)	1	1.61 (3.67)	7.9 (9.8)	5	5.5 (1.6)	0.15 (0.82)	256 (29)	-6.7 (-2.9) <sup>b</sup>	71 (24)	1.7 (0.15)	23 (6.6)	2.0 (1.0)	
CN Aβ+	21	12:9	76.0 (3.4)	16.1 (3.3)	10	1.07 (2.21)	6.6 (5.2)	11	6.4 (1.6)	0.52 (0.89) <sup>c</sup>	151 (26) <sup>b</sup>	-3.3 (-1.5) <sup>d</sup>	86 (33) <sup>d</sup>	1.6 (0.21)	31 (10) <sup>d</sup>	3.4 (1.8)	
AD Aβ+	15	6:9	73.0 (6.3)	15.0 (2.9)	12	0.35 (0.33)	7.6 (9.2)	6	15.4 (5.1) <sup>b,e</sup>	5.10 (2.80) <sup>b,e</sup>	126 (20) <sup>b,f</sup>	0.1 (1.2)	114 (57) <sup>d,f</sup>	1.5 (0.31)	36 (9.1) <sup>b,f</sup>	4.2 (1.5) <sup>c,f</sup>	

Abbreviations: Aβ, β-amyloid; AD, Alzheimer disease; AD Aβ+, Aβ-positive AD group; APOE, apolipoprotein E; CN, cognitively normal; CN Aβ+, Aβ-positive CN group; CN Aβ-d, declining Aβ-negative CN group; CN Aβ-s, stable Aβ-negative CN group; ng/L\*<sup>b</sup>, change in concentration per year; WM Hypertensities, white matter hypertensities (volume in standardized space, corrected for head size).

<sup>a</sup>For group comparisons of demographic factors, Kruskal-Wallis test was used for age ( $P = .10$ ), education ( $P = .20$ ), white matter hypertensities ( $P = .81$ ), and history of hypertension ( $P = .84$ ). Data for Aβ42 level, T-tau level, and cognitive subscale score on the Cognitive Subscale of the Alzheimer Disease Assessment Scale are modeled intercepts (baseline levels) and slopes from linear mixed-effects models, adjusted for age and sex (Aβ42 levels were modeled separately for cognitively normal control subjects and patients with Alzheimer disease dementia because of different distributions). Group comparisons for Aβ42 level, T-tau level, P-tau level, and cognitive subscale score on the Cognitive Subscale of the Alzheimer Disease Assessment Scale were performed by comparing every group with the CN Aβ-s group and comparing the AD Aβ+ group with the CN Aβ+ group in the linear mixed-effects models.

<sup>b</sup> $P < .001$  vs the CN Aβ-s group.

<sup>c</sup> $P < .05$  vs the CN Aβ-s group.

<sup>d</sup> $P < .01$  vs the CN Aβ-s group.

<sup>e</sup> $P < .001$  vs the CN Aβ+ group.

<sup>f</sup> $P < .05$  vs the CN Aβ+ group.